

Deep defects in narrow-gap semiconductors

W. Li and J. D. Patterson

Physics and Space Sciences Department, Florida Institute of Technology, Melbourne, Florida 32901-6988

(Received 16 March 1994; revised manuscript received 7 July 1994)

We use a Green's-function technique to calculate the position of deep defects in narrow-gap semiconductors. In order to predict chemical trends, we examine the effects of several different chemical elements. Substitutional (including antisite), (ideal) vacancy, and interstitial (self and foreign) deep defects are considered. The compounds considered are mercury cadmium telluride (MCT), mercury zinc telluride (MZT), and mercury zinc selenide (MZS). The effect of relaxation of neighbors is considered for the substitutional and interstitial cases. Relaxation effects can be greater for the interstitial case than for the substitutional one. For all cases we find deep defects in the energy gap only for cation-site *s*-like orbitals or anion-site *p*-like orbitals, and for the substitutional case only the latter are appreciably effected by relaxation. For substitutional impurities in MCT, MZT, and MZS, we consider x (the concentration of Cd or Zn) in the range $0.1 < x < 0.3$ and also for both the substitutional and interstitial cases we do extensive calculations for x values appropriate to a band gap of 0.1 eV. Specific results are given in figures and tables and comparison to experiment and other calculations is made in a limited number of cases. For the substitutional case we find that I, Se, S, Rn, and N are possible defect candidates to form cation-site, *s*-like levels in MCT, and Zn and Mg are for anion-site, *p*-like levels. Similarly, in MCT for the interstitial case we find deep defect levels in the band gap for Au, Ag, Hg, Cd, Cu, and Zn for the cation site, and N, Ar, O, and F for the anion site. For the substitutional cases we have some examples where relaxation moves the levels into the band gap, whereas for interstitial cases we have examples where relaxation moves them out of the band gap. We find that the chemical trends of defect levels in MZT are similar to that in MCT. However, the same conclusion does not hold for MZS. We have also used perturbation theory (see the Appendix) to look at the effect of nonparabolicity on shallow donor levels, and find it can increase the binding by 10% or so. Although the absolute accuracy of our results is limited, the precision is good, and hence chemical trends are accurately predicted. Further work involves calculating the effect of charged-state interactions and the effect of relaxation on vacancy levels.

I. INTRODUCTION

The study of point defects in semiconductors has a long history.¹⁻³ In particular, the detailed understanding of shallow defects in common semiconductors traces back to the classic work of Kohn and Luttinger,² and can be regarded as basically understood. However, the study of defects in narrow-gap semiconductors represents a much less clear story. Here both shallow defects (caused by long-range potentials) and deep defects (from short-range potentials) are far from being completely understood.

Narrow-gap semiconductors find important application for infrared detectors. Typical ones such as mercury cadmium telluride (MCT) and mercury zinc telluride (MZT) are difficult to grow uniformly under the stress of gravity induced convection, and hence are of interest to NASA for growth in microgravity. These semiconductors have nonparabolic bands, and they are particularly interesting because they have large mobilities and band gaps with corresponding absorption frequencies in the infrared.

In order to evaluate a specific growth technique, one needs to evaluate the perfection of the crystal. Until one can identify and characterize the defects, it is impossible to make accurate statements about the degree of crystal perfection. Further, a full characterization of crystal perfection involves not only a theoretical study of all com-

mon defects, but also experimental verification of the proposed models.

The main defects we will look at are deep defects caused by short-range potentials. We will consider substitutional (including antisite), vacancy, and interstitial (self and foreign) deep defects. For substitutional and interstitial impurities, the effects of relaxation are included. Of particular interest is which substitutional and interstitial impurities produce energy levels in the band gap. In the Appendix, some brief results will be given for shallow defects caused by long-range potentials, where perturbation theory will be used to look at the effects of nonparabolic bands.

The energy levels of deep defects may or may not be near the band edge. Deep defects are often very important as recombination centers and they control lifetime and noise, but they may also be donors or acceptors; hence they have an important effect on the electronic properties of crystals. Shallow defects have energy near the band edge, and in narrow-gap semiconductors shallow defects are often assumed to be fully ionized. Their main importance is in supplying carriers, but like all defects they may also scatter the carriers.

In this study, all results are calculational and our focus is on the chemical trends of deep energy levels in narrow-gap semiconductors. As is standard, the Green's-function technique will be used to calculate the

energy levels of the deep defects. We start in Sec. II with a summary of that method for the substitutional and ideal vacancy cases. In Sec. III, we discuss relaxation effects for interstitial impurities. In Sec. IV, we note how to modify our techniques for interstitial defects. In Sec. V, we make some comparison to experiment. In the Appendix, we present some brief perturbation theory results for shallow donor impurities. Experimentally both shallow impurities and deep defects may produce energy levels near a band edge, so it can be difficult to separate them experimentally.

II. GREEN'S-FUNCTION METHODS

A. General results

The general formulation, determination of the impurity potential,⁴⁻⁶ and determination of the perfect crystal function Green's function,⁵⁻⁷ as well as how these are used to calculate defect energy levels, are well discussed in the literature. We should mention, however, that the idea of a perfect crystal for these ternary alloys assumes a virtual-crystal approximation (VCA) in which the effect of the local environment is lost. Li and Poltz⁸ have noted that alloy disorder can be treated beyond the VCA by using a recursion method. The ideal vacancy model is also discussed in the literature⁹ as a limiting case of a substitutional impurity, and assumes a vacancy is formed by removing an atom from the crystal, but leaving all other atoms in the same position. This means that relaxation is excluded.

We also should make a comment about the effects of spin. Unlike III-V semiconductors, II-VI semiconductors may have a strong spin-orbit coupling, which must be and is included in the band-structure calculations we use. Based on the band-structure theory of Vogl, Hjalmarson, and Dow,⁷ Kobayashi, Sankey, and Dow¹⁰ proposed a theory for II-VI semiconductors which includes spin-orbit coupling. The situation for the part of the Hamiltonian that describes the defect is different. The spin-orbit interaction is weak and can be neglected, so that including the degeneracy due to spin just doubles the degeneracy of each level and the Hjalmarson theory is still valid.

B. Lattice relaxation and molecular-dynamics approach

The formulation of the theory we will use here has already been fully reported in the literature,¹¹⁻¹⁴ so we just summarize some pertinent facts here. Only the off-diagonal elements of the defect potential matrix are related to bond length, and when these elements are set equal to zero the effects of lattice relaxation are excluded. The off-diagonal elements are determined by parameters α_i , which are given by

$$\alpha_i = -c_i \left[\frac{1}{d_I^2} - \frac{1}{d_H^2} \right], \quad (1)$$

where d_I is the bond length between the defect and the nearest neighbors, d_H is the bond length of the host crystal, and c_i is a proportionality constant which depends on

i and on the host materials.¹¹ Note that the sign of α_i determines the direction of lattice relaxation. In order to determine α_i , we need only determine d_I , since d_H is known. This is accomplished by molecular dynamics in the way already published.¹¹⁻¹⁴

III. INTERSTITIAL DEFECTS AND RELAXATION

Interstitials are an important kind of point defect in semiconductors. Self-interstitial impurities and vacancies are the most common native defects in semiconductors. We study tetrahedral-site s - and p -bonded interstitial impurities in MCT, MZT, and mercury zinc selenide (MZS). The hexagonal interstitial configuration can probably also be treated by a similar model to that which we use, but it is not considered here. The situation of tetrahedral-site interstitial impurities is different from substitutional defects in the zinc-blende structure. The symmetry is the same, but the four nearest-neighbor impurities have six next-nearest impurities which are only 15% further rather than 12 which are 66% further. Sankey and Dow¹⁵ have proposed a model to calculate deep levels introduced by an s - and p -bonded impurity occupying an interstitial site of tetrahedral symmetry in Si. To extend this model, the host Hamiltonian is now determined by the band-structure theory proposed by Kobayashi, Sankey, and Dow,¹⁰ and the rest of the model will be the same as Sankey's model.

IV. RESULTS AND DISCUSSION

Our results are for the narrow-gap semiconductors MCT ($\text{Hg}_{1-x}\text{Cd}_x\text{Te}$), MZT ($\text{Hg}_{1-x}\text{Zn}_x\text{Te}$), and MZS ($\text{Hg}_{1-x}\text{Zn}_x\text{Se}$). Many of our results are quite similar and are summarized in Tables I-III for the case of $E_g = 0.1$ eV (so $x = 0.22$ for MCT, 0.15 for MZT, and 0.08 for MZS).

We start our discussion by looking at how deep levels vary as a function of x for the substitutional case without relaxation. Figure 1 shows that Mg, Zn (antisite), and Cd form anion-site, p -like deep levels in the band gap of MZT provided x is not too small. Note that Cd does not form a deep level for $E_g < 0.1$ eV. By looking at these and results of similar calculations, we find that the slopes of the deep levels dE/dx are always smaller than dE_{gap}/dx . This means that if the level is in the gap for x_0 then it is for all x ; $x_0 < x < 1$ (provided also $dE/dx > 0$ which is common). This has important consequences, as it is much easier to detect deep levels in wide-gap semiconductors. We also find that the slopes of the anion-site deep levels are very small. We characterize this by saying they are "attached" to the valence level. This feature holds for the deep levels in MCT and MZS.

In Fig. 2, we display results of similar calculations for substitutional deep levels in MZT with $E_g = 0.1$ eV for cation-site, s -like levels. A few levels which are resonant (above the conduction-band edge or below the valence-band edge) are also shown; this is because the effects of relaxation or other effects may easily shift these levels (into or perhaps further out of the band). Energetic considerations indicate why anion-site p levels (with electron

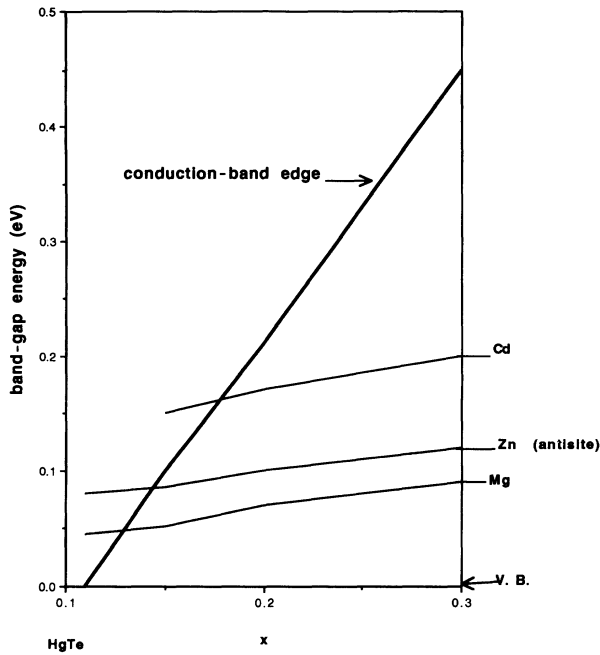


FIG. 1. Substitutional deep levels in MZT as a function of x (anion site, p -like).

clouds near + cation sites) and cation-site s levels (with electron clouds far from - anion sites) would be the only cases found to produce deep levels.

We find, as expected, that impurities from rows to the right of the cation atoms in the Periodic Table form donorlike substitutional impurities because they are more electronegative, while impurities to the left of the anion atoms form acceptorlike substitutional impurities. We also find that although the same impurities form different energy levels in different materials, the order of these levels in the materials is the same. For example, the order of deep levels produced by impurities of Mg, Zn, and Cd substitutional for anion atom Te in MCT is $E_{Mg} < E_{Zn} < E_{Cd}$. The same order is found in MZT and MZS. Therefore, if we can experimentally determine one deep level produced by a specific impurity, we can then, based on calculations, predict the positions of deep levels produced by other impurities. This is really what we mean when we say we can predict chemical trends.

We illustrate how we treat relaxation with Fig. 3. The parameter α is involved in the off-diagonal parts of the defect potential, and can be determined from the results of the molecular-dynamics calculation; $\alpha=0$ corresponds to no relaxation. The on-diagonal parts of the defect potential determine the "impurity potential" of Fig. 3, where we have noted its value for Mg. The intersection of the vertical Mg line with the $\alpha=0$ line determines the predicted defect level without relaxation. The intersection of the line with the appropriate value of α determined the defect level with relaxation. If there is no intersection for the predicted value of α , then there is no predicted deep level. Typically, relaxation directions are opposite for A_1 and T_2 states for the same value of α , and not symmetrical (e.g., in Fig. 4, $\alpha_{T_2}=0.4$ corre-

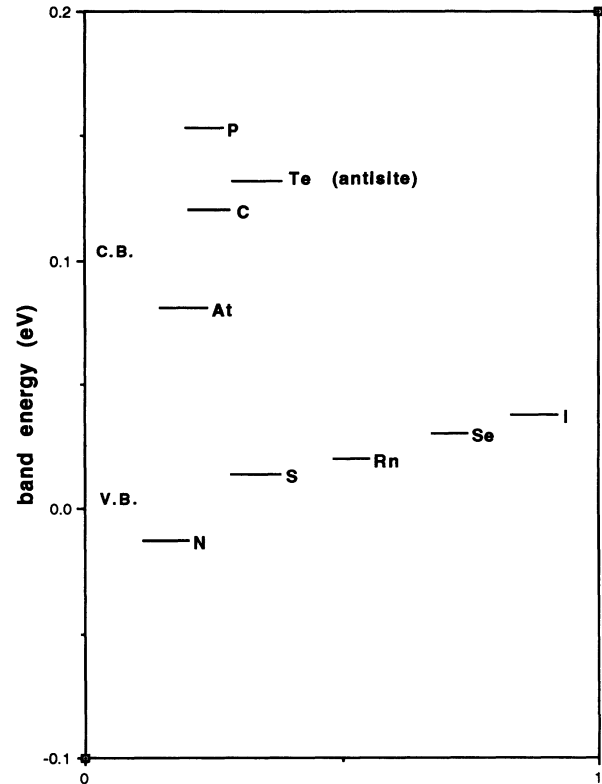


FIG. 2. Substitutional deep levels in MZT for $E_g=0.1$ eV (cation site, s -like).

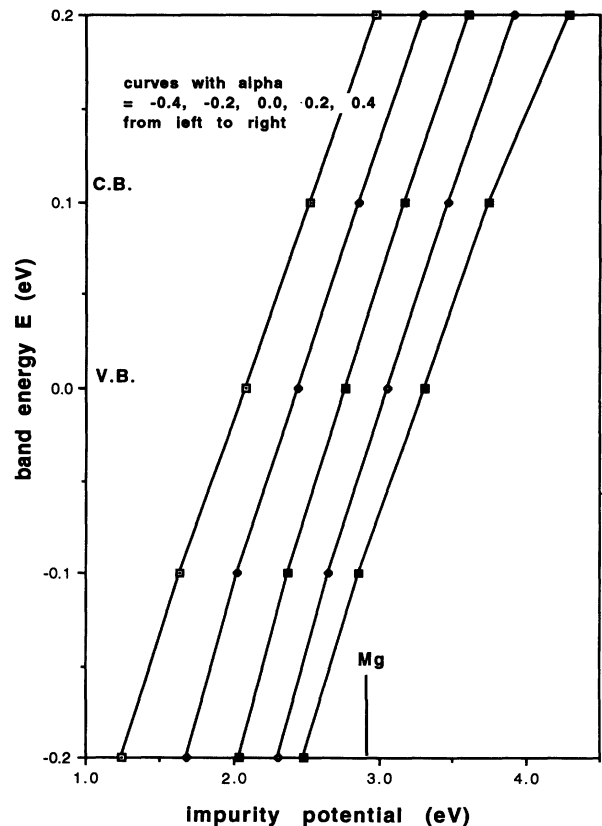


FIG. 3. Substitutional deep levels in MZT for $E_g=0.1$ eV with lattice relaxation (anion site, p -like).

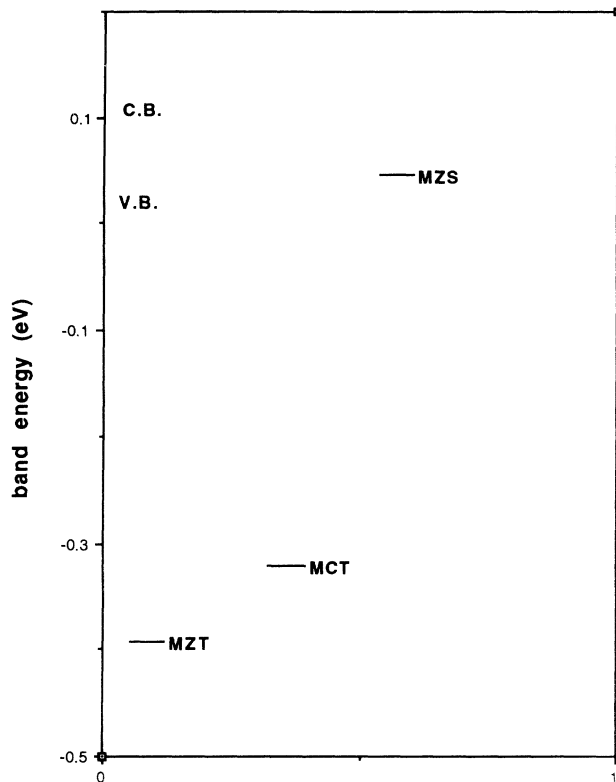


FIG. 4. Vacancy deep levels for $E_g = 0.1$ eV (cation site, s -like).

sponds to 20% inward relaxation, while $\alpha_{T_2} = -0.4$ corresponds to 48% outward relaxation). We have only shown the effect of relaxation on p -levels because relaxation on s levels is so small that it can be neglected as far as its effects in deep levels goes. We find that this result is in conflict with the results of IV and III-V materials

where the lattice relaxation is sensitive to the A_1 levels.^{13,14} From an inspection of the calculations, we believe that this conflict is due to the different properties of the band structures between IV and III-V materials and the II-VI materials of interest. This result may be explained by the fact that the "impurity potential" of the s level is often much larger than that of p level for the same impurity in the case of II-VI materials. Also, the chemical trend for the $\alpha \neq 0$ curves is similar to those for $\alpha = 0$.

Note also that $\alpha_{T_2} > 0$ moves deep levels toward the valence band, and $\alpha_{T_2} < 0$ moves them toward the conduction band. The effects of lattice relaxation can easily move levels into or out of the band gap. The effects of lattice relaxation on substitutional deep levels for all the calculations we have done are summarized in Table I, where we have assumed $E_g = 0.1$ eV for uniformity. Only anion-site p -like levels are shown in Table I, as relaxation does not effect cation-site s -like levels. For completeness in Table II we give our predicted levels for substitutional cation-site s -like levels. Typical lattice relaxations for the substitutional case are in the range of 4–6.5 %, resulting in shifts of typically less than $E_g/2$, so defects that are predicted to be in the middle of the gap before relaxation tend to stay in the gap.

Deep levels produced by vacancies in MCT, MZT, and MZS are summarized in Fig. 4, which shows the cation-site, s -like vacancies levels of MCT, MZT, and MZS. The vacancy levels of MCT and MZT are resonant in the valence band, and the vacancy level of MZS is in the middle of the band gap. The anion-site, p -like vacancy levels are slightly below the corresponding levels in Fig. 4 and are not shown. These levels are calculated by "the ideal vacancy model" already mentioned. Since the effects of lattice relaxation are not included in the calculation, the accuracy of these levels needs to be improved.

Typical results for interstitial deep levels without relax-

TABLE I. Effects of lattice relaxation on substitutional deep levels.

System	d_H (Å)	d_I (Å)	$Dx = d_I - d_H$	% of relaxation	Deep levels ^a	
					(no relax)	(relaxed)
MCT: Cd _{Te} ^b	2.8	2.97	0.17	6.1	C.B. ^c	C.B.
MCT: Mg _{Te}	2.8	2.96	0.16	5.7	$0.3E_g$ ^d	$0.5E_g$
MCT: Zn _{Te}	2.8	2.98	0.18	6.4	$0.5E_g$	$0.9E_g$
MCT: Hg _{Te} ^b	2.8	2.97	0.17	6.1	C.B.	C.B.
MZT: Zn _{Te} ^b	2.74	2.61	-0.13	4.7	$0.98E_g$	$0.7E_g$
MZT: Mg _{Te}	2.74	2.60	-0.14	5.1	$0.5E_g$	$0.3E_g$
MZT: Cd _{Te}	2.74	2.60	-0.14	5.1	C.B.	C.B.
MZT: Hg _{Te} ^b	2.74	2.60	-0.14	5.1	C.B.	C.B.
MZS: Be _{Se}	2.62	2.74	0.12	4.6	$0.3E_g$	$0.6E_g$
MZS: Tl _{Se}	2.62	2.77	0.15	5.7	$-0.1E_g$	$0.4E_g$
MZS: In _{Se}	2.62	2.77	0.15	5.7	$-1.1E_g$	$0.3E_g$
MZS: Hg _{Se} ^b	2.62	2.73	0.11	4.2	C.B.	C.B.
MZS: Zn _{Se} ^b	2.62	2.73	0.11	4.2	C.B.	C.B.

^aAll deep levels in this table are anion-site, p -like deep levels.

^bAll these are antisite impurities.

^cC.B. means conduction band.

^d E_g means energy band gap.

TABLE II. Cation site, *s*-like substitutional levels.

Systems	Deep levels
MCT:Br	$0.01E_g$
MCT:N	$0.14E_g$
MCT:S	$0.52E_g$
MCT:Rn	$0.55E_g$
MCT:Se	$0.87E_g$
MCT:I	$0.92E_g$
MZT:N	$-0.1E_g$
MZT:S	$0.15E_g$
MZT:Rn	$0.21E_g$
MZT:Se	$0.27E_g$
MZT:I	$0.42E_g$
MZT:At	$0.82E_g$

ation are shown in Fig. 5. Our complete interstitial results with and without relaxation are shown in Table III. In all of these, "cation site" means that the nearest neighbors of the interstitials are anion atoms, and "anion site" means the nearest neighbors of the interstitials are cation atoms.

We only consider breathing-mode distortions for interstitial impurities. At this time we have not yet included Jahn-Teller distortions, which are symmetry-breaking distortions. Therefore, the breathing-mode distortions are only a first-order approximation for realistic calculations.

Since we only consider tetrahedral interstitial impurities, an interstitial impurity will have four neighbors. In our calculations we consider two types of self-interstitials.

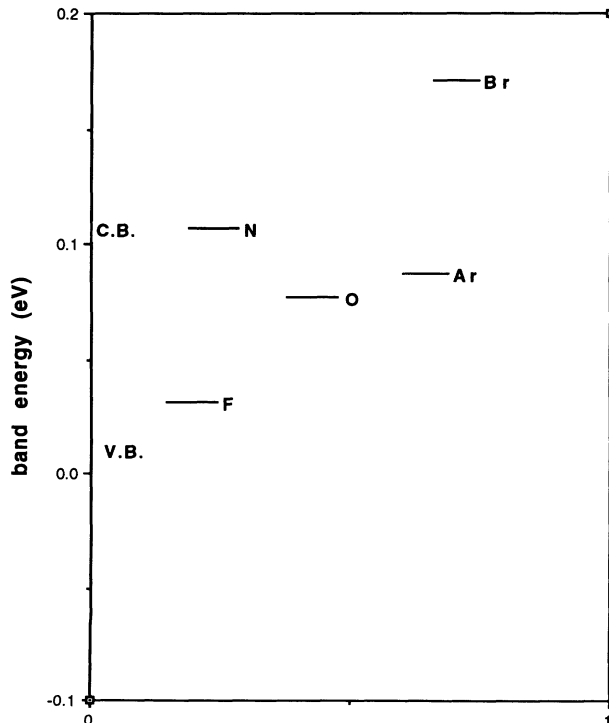


FIG. 5. Interstitial deep levels in MZT for $E_g = 0.1$ eV (anion site, *p*-like).

One type is the cation atoms in cation sites, and another is the anion atoms in anion sites. Therefore we can use the definitions of donorlike deep levels and acceptorlike deep levels similar to the case of substitutional impurities. For example, in the case of MCT, consider a Cd atom in a cation site. This self-interstitial will produce a deep level. If an impurity comes from rows to the right of Cd in the Periodic Table, then we say that this impurity will form a donorlike deep level in MCT.

There are some interesting comments one can make for the predictions without relaxation. Cation-site *s*-like self-interstitials often produce deep levels in the energy-band gap. For example, for MCT, both self-interstitial impurities Hg and Cd produce deep levels well within the band gap. In contrast to the deep levels produced by substitutional impurities, the cation-site deep levels produced by interstitials are often acceptorlike. On the other hand, the anion-site interstitial deep levels can be donorlike or acceptorlike.

The effects of relaxation for the interstitial case are seen in Table III. In Table III all interstitial impurities are divided into two groups: cation-site interstitials and anion-site interstitials. For each material the first group in Table III is cation-site interstitials and the second group is anion-site interstitials. From Eq. (1) the values of α can be obtained easily with appropriate c_i , therefore we did not show the results of α in Table I and III. Similar comments to those made for the substitutional case apply here. Relaxation can range from 0.0–16 % and may cause the level to move into or out of the band gap.

Through the calculations we can conclude that the chemical trends of defects levels in MZT is similar to that in MCT. They have almost the same slopes of deep levels as a function of x for the same defects in both cation-site, *s*-like and anion-site, *p*-like cases. They have similar ranges of the impurity potential for the same impurity site and symmetry. That is, if we predict a deep level in the band gap for appropriate site and symmetry in MCT, most likely this deep level will be predicted in the band gap or near the band gap for the same site and symmetry in MZT. In addition, the effects of lattice relaxation on deep levels in both materials are almost the same. However, even though some characteristics of deep levels in MZS are similar to those in MCT and MZT, generally speaking the chemical trends of deep levels in MZS are not the same as those in MCT and MZT.

V. FURTHER DISCUSSION AND COMPARISON TO EXPERIMENT

Many experimental techniques can be used to study the properties of defects in narrow-gap semiconductors, and especially to detect energy levels in the band gap. These techniques include photoluminescence (PL),¹⁶ deep level transient spectroscopy (DLTS),¹⁷ electron paramagnetic resonance (EPR),¹⁸ and several others. The details of the techniques can be understood from these references. Detecting the defects and identifying them with a model is not easy. In the last two decades, much effort has been devoted to MCT,¹⁰ but relatively little has been done on MZT and MZS.¹⁹ Some experimental results which are

firmly identified for MCT are shown and compared with our predicted levels in Table IV. In this table all experimental data are from samples with alloy composition x in the range of $0.2 < x < 0.3$. We know that when x is changed, the width of the band gap is also changed. Therefore the position of a deep level will be changed for different values of x . However, since the range of x is small, and the data are given by relative positions in the band gap, we believe that any fluctuation due to x variation is in the range of the experimental error and therefore the comparison is reasonable. In the second and third rows of the table, the experimental data indicates that a Te interstitial or an antisite Te atom may produce a deep level in the band gap, but there is not enough evidence to identify which point defect produces the deep

level. We make theoretical predictions for both point defects in the table. The last two rows in the table show a similar situation. Our results favor the point defect being interstitial Au*. We believe that more reliable experiment data, especially the data for MZT and MZS, will help us to understand the problem better. Our results compare favorably with experiment for the case shown in Table IV. Other comparisons, where the levels are not as clearly identified, lead us to say we are never in error by more than say 0.15 eV or more than can be accounted for by, say, charged-state splitting,²⁰ and the calculation *vis a vis* relative positions of levels is much more accurate, i.e., the chemical trends really are preserved.

We should also mention that our results compare favorably with other calculations, which also typically do

TABLE III. Effects of lattice relaxation on interstitial deep levels.

System	$d_H(A)$	$d_I(A)$	$Dx = d_I - d_H$	% of relaxation	Deep levels ^a	
					(no relax)	(relaxed)
MCT: Cd ^d	2.8	2.94	0.12	4.3	$0.74E_g^c$	$0.77E_g$
MCT: Mg	2.8	3.10	0.24	8.6	$0.98E_g$	C.B. ^d
MCT: Zn	2.8	2.81	0.01	0.3	$0.1E_g$	$0.1E_g$
MCT: Hg ^b	2.8	2.90	0.10	3.6	$0.82E_g$	$0.83E_g$
MCT: Au	2.8	2.90	0.10	3.6	$0.9E_g$	$0.91E_g$
MCT: Ag	2.8	2.91	0.11	3.9	$0.87E_g$	$0.88E_g$
MCT: Cu	2.8	2.91	0.11	3.9	$0.2E_g$	$0.22E_g$
MCT: Te ^b	2.8	2.95	0.15	5.4	C.B.	C.B.
MCT: N	2.8	2.56	-0.24	8.6	$0.9E_g$	$0.7E_g$
MCT: O	2.8	2.54	-0.26	9.3	$0.8E_g$	$0.6E_g$
MCT: Ar	2.8	2.59	-0.21	7.5	$0.82E_g$	$0.62E_g$
MCT: F	2.8	2.52	-0.28	10	$0.44E_g$	$0.24E_g$
MZT: Zn ^b	2.74	2.92	0.18	6.6	V.B. ^d	$0.04E_g$
MZT: Mg	2.74	2.80	0.06	2.2	$0.9E_g$	$0.91E_g$
MZT: Cd	2.74	2.82	0.08	2.9	$0.6E_g$	$0.61E_g$
MZT: Hg ^b	2.74	2.81	0.07	2.5	$0.68E_g$	$0.69E_g$
MZT: Au	2.74	2.80	0.06	2.2	$0.74E_g$	$0.55E_g$
MZT: Ag	2.74	2.80	0.06	2.2	$0.70E_g$	$0.71E_g$
MZT: Cu	2.74	2.88	0.14	5.1	$0.18E_g$	$0.30E_g$
MZT: Te ^b	2.74	2.35	-0.41	15	C.B.	C.B.
MZT: N	2.74	3.10	0.36	13	C.B.	C.B.
MZT: O	2.74	3.14	0.40	14.6	$0.8E_g$	C.B.
MZT: Ar	2.74	3.15	0.41	15	$0.9E_g$	C.B.
MZT: F	2.74	3.18	0.44	16	$0.3E_g$	$0.5E_g$
MZS: Hg ^b	2.62	2.71	0.09	3.4	$0.98E_g$	C.B.
MZS: Zn ^b	2.62	2.78	0.16	6.1	$0.04E_g$	$0.14E_g$
MZS: Cd	2.62	2.72	0.10	3.8	$0.86E_g$	$0.88E_g$
MZS: Cu	2.62	2.75	0.13	5.0	$0.24E_g$	$0.34E_g$
MZS: Ag	2.62	2.71	0.09	3.4	C.B.	C.B.
MZS: Se ^b	2.62	2.58	-0.04	1.5	C.B.	C.B.
MZS: N	2.62	2.61	-0.01	0.0	C.B.	C.B.
MZS: O	2.62	2.37	-0.25	9.5	$0.98E_g$	C.B.
MZS: F	2.62	2.51	-0.11	4.2	$0.50E_g$	$0.40E_g$

^aAll deep levels in this table are either anion-site, p -like deep levels or cation-site, s -like deep levels. All interstitials are on the preferred positions.

^bAll these are self-interstitials.

^c E_g means energy-band gaps.

^dC.B. means conduction-band edge and V.B. means valence-band edge.

TABLE IV. Comparison of the predicted deep levels in MCT with experimental data.

System	Deep levels	
	Experiment	Theory ^f
Hg _I ^a (donor)	0.7E _g ^b (Ref. 18)	0.83E _g
Te _I ^a (recom) ^c	0.4E _g (Refs. 18 and 28)	E _c ^d +0.1 eV ^e
Te _{Hg} (recom)	0.4E _g (Refs. 18 and 28)	E _c +0.06 eV ^e
Cu _{Te} (donor)	0.5E _g (Ref. 29)	E _c +0.06 eV ^e
Cu _{Te} (donor)	E _c +0.05 eV (Ref. 18)	E _c +0.06 eV ^e
Au _{Te} (donor)	0.8E _g (Refs. 18 and 29)	E _c +0.04 eV ^e
Au _I ^a (donor)	0.8E _g (Refs. 18 and 29)	0.91E _g

^aThese are interstitial impurities.

^bE_g means energy band gap.

^cRecombination center.

^dE_c means conduction-band edge.

^eThe difference between data and the theory result can be explained by the effects of charged-state splitting.

^fThe *x* values for the experimental data here are in the range 0.2 < *x* < 0.3. For our calculations, *x* = 0.22. As seen in Fig. 1, the change in the energy levels for 0.2 < *x* < 0.3 is very small and can be ignored for rough comparisons.

not predict absolute energies with accuracy, but which do predict chemical trends. Berding, von Schilfgaard, and Sher²¹ have made predictions for the effects of lattice relaxation on substitutional impurities in HgTe. They found that for the composition *x* = 0, a Hg antisite defect (in a Te site) and a Te antisite defect (in a Hg site) in HgTe introduce 0.06 and 0.2 Å outward relaxation, respectively. In our calculation we found the corresponding relaxations are 0.05 and 0.13 Å. Interstitial impurities in MCT have been studied by Morgan-Pond, Goettig, and Schick.²²⁻²⁴ They predict that Cd, Hg, and In interstitials in MCT have 3-4 % relaxation, while we predict Cd and Hg interstitials in MCT have 4.3 and 3.6% relaxation, respectively. Their predictions for an *s*-like level in the band gap due to a Hg interstitial, and for an In interstitial resonant in the valence band, also agree with ours.

In summary, our defect energy level results, which include relaxation of neighbors, are useful because they bear on the electronic characterization of real materials used for real devices such as infrared detectors. The chemical trends of the levels are usefully predicted, but absolute accuracy requires the inclusion of charged-state interactions (where relevant), and, in the case of vacancies, the relaxation of neighbors needs to be added, as we have already done for the other cases.

In the first column of the table we give a suggested characterization of deep levels as given by experiments. Interested readers can find detailed discussions in the references cited. However, based on our theory, the characteristics of deep levels are not unique. For example, the deep levels produced by Te_{Hg}, Cu_{Te}, and Au_I can be either donorlike or acceptorlike. In Table IV we give only the experimental assignment.

ACKNOWLEDGMENTS

This work was supported by NASA/Marshall Space Flight Center Grant No. NAG8-941. We appreciate the counsel of Dr. S. L. Lehoczky of MSFC.

APPENDIX: RESULTS FOR SHALLOW LEVELS IN II-VI MATERIALS

Although this is a paper on deep defects (defined as arising from short-range potentials), some comments on shallow defects and especially the Coulomb tail are still appropriate. Our calculation may be fairly accurate for neutral deep defects whose energies are near the center of the gap. Even this relatively weak statement is called into question by the fact that the central cell potential tends to localize the wave function where the magnitude of the Coulomb tail is greatest. Also, the Coulomb tail is undoubtedly important for charged states. In fact it has been shown quantitatively²⁵ that a central cell potential, which by itself does not cause binding, and a Coulomb tail together can cause significant binding, far greater than an estimate based on the effective-mass equation. In addition, for energies near the band edge, we are still using only the central cell potential, and for these the Coulomb tail is certainly important. Thus our deep defect calculations that yield energy levels near the band edges are intrinsically not very accurate because of the neglect of the Coulomb tail; hence we thought it would be interesting to look at shallow defects (which include only the Coulomb tail) in narrow-gap semiconductors, and in particular look at the effect of nonparabolicity on these energy levels. The situation is complicated by many factors besides nonparabolicity. These include screening, site dependence, central cell corrections, alloy disorder, lattice coupling, lattice relaxation, impurity interactions, and band coupling and degeneracy. Because of these complications, shallow levels, e.g., donors, are often considered just to be fully ionized at all temperatures of interest. To evaluate all these factors would take us far beyond the present paper. We confine ourselves to the effect of band nonparabolicity.

The Hamiltonian that corrects for nonparabolic behavior is²⁶

$$H^1 = ap^2 + bp_z\phi p_z + cp_+ \phi p_- + dp_- \phi p_+, \quad (\text{A1})$$

where *p* is the momentum operator and ϕ is the hydrogenic potential. The coefficients *a*, *b*, *c*, and *d* are given by Bastard.²⁶ Using appropriate values for the parame-

TABLE V. Predicted energies for shallow donors in II-VI materials.

	MCT	MZT
<i>P</i> (momentum matrix elements)	1.290 × 10 ¹⁹ eV cm / erg sec	1.238 × eV cm / erg sec
<i>x</i>	0.19	0.13
<i>k</i> (dielectric const)	17.56	18.35
Δ (spin-orbit splitting)	1.05 eV	0.9 eV
E _g	0.1 eV	0.1 eV
E _{ground} ^{donor}	-0.0101 eV	-0.0099 eV
ΔE	-0.00135 eV	-0.00125 eV
$\left \frac{\Delta E}{E_{\text{gap}}} \right $	1.35%	1.25%
$\left \frac{\Delta E}{E_{\text{ground}}^{\text{donor}}} \right $	-13.4%	-12.6%

ters²⁷ for MCT and MZT, we can evaluate E_{gap} , E_{donor} , the ground-state energy, and the ground-state donor wave function ψ_0 . To first order, the energy change is given by

$$\Delta E = \langle \psi_0 | H^1 | \psi_0 \rangle . \quad (\text{A2})$$

Our results are given in Table V. Interestingly, the results predicted an approximate 10% downward shift in binding energy due to the effect of nonparabolicity. From this aspect, the Coulomb tail is more effective in binding (e.g., donor states) in nonparabolic than parabolic semiconductors.

-
- ¹S. T. Pantelides, *Deep Centers in Semiconductors*, 2nd ed. (Gordon and Breach, Yverdon, Switzerland, 1992).
- ²S. T. Pantelides, *Rev. Mod. Phys.* **50**, 797 (1978).
- ³M. Lannoo and J. Bourgoin, *Point Defects in Semiconductors I: Theoretical Aspects* (Springer-Verlag, Berlin, 1981).
- ⁴E. N. Economou, *Green's Function in Quantum Physics* (Springer-Verlag, Berlin, 1990).
- ⁵H. P. Hjalmarson, P. Vogl, D. J. Wolford, and John D. Dow, *Phys. Rev. Lett.* **44**, 810 (1980).
- ⁶H. P. Hjalmarson, Ph.D. thesis, The University of Illinois, 1979.
- ⁷P. Vogl, H. P. Hjalmarson, and J. D. Dow, *J. Phys. Chem. Solids* **44**, 365 (1983).
- ⁸Z. Q. Li and W. Potz, *Phys. Rev. B* **46**, 2109 (1992).
- ⁹S. Das Sarma and A. Madhukar, *Phys. Rev. B* **24**, 2051 (1981).
- ¹⁰A. Kobayashi, O. F. Sankey, and J. D. Dow, *Phys. Rev. B* **25**, 6367 (1982).
- ¹¹W. Li and C. W. Myles, *Phys. Rev. B* **43**, 2192 (1991). See also J. Shen, S. Y. Ren, and J. D. Dow, *ibid.* **42**, 9119 (1990).
- ¹²W. Li and C. W. Myles, *Phys. B* **43**, 9947 (1991).
- ¹³W. Li and C. W. Myles, *Phys. Rev. B* **47**, 4281 (1993).
- ¹⁴W. Li, Ph.D. thesis, Texas Tech University, 1991.
- ¹⁵O. F. Sankey and J. D. Dow, *Phys. Rev. B* **27**, 7641 (1983).
- ¹⁶D. L. Polla and R. J. Aggarwal, *Appl. Phys. Lett.* **44**, 775 (1984).
- ¹⁷V. A. Cotton, J. A. Wilson, and C. E. Jones, *J. Appl. Phys.* **58**, 2208 (1985). See also M. C. Chen, M. W. Goodwin, and T. L. Polgreen, *J. Cryst. Growth* **86**, 484 (1988).
- ¹⁸C. E. Jones, K. James, J. Merz, R. Braunstein, M. Burd, M. Eetemadi, S. Hutton, and J. Drumheller, *J. Vac. Sci. Technol. A* **3**, 131 (1985).
- ¹⁹A. Seyni, R. Granger, R. Triboulet, S. Rolland, and A. Lasbely, *Phys. Status Solidi A* **128**, K27 (1991).
- ²⁰C. W. Myles, *J. Vac. Sci. Technol. A* **6**, 2675 (1988).
- ²¹M. A. Berding, M. van Schilfgaarde, and A. Sher, *J. Vac. Sci. Technol. B* **10**, 1471 (1992).
- ²²J. T. Schick and C. G. Morgan-Pond, *J. Vac. Sci. Technol. A* **8**, 1108 (1990).
- ²³S. Goettig and C. G. Morgan-Pond, *J. Vac. Sci. Technol. A* **6**, 2670 (1988).
- ²⁴S. Goettig and C. G. Morgan-Pond, *Phys. Rev. B* **42**, 11 743 (1990).
- ²⁵D. J. Lohrmann *et al.*, *Phys. Rev. B* **40**, 8404 (1989); **40**, 8410 (1989).
- ²⁶G. Bastard, *Wave Mechanics Applied to Semiconductor Heterostructures* (Halstead, New York, 1988), p. 59.
- ²⁷J. D. Patterson, W. Gobba, S. L. Lehoczky, *J. Mater. Res.* **7**, 2211 (1992).
- ²⁸A. Sher, M. A. Berding, M. Van Schilfgaarde, and An-Ban Chen, *Semicond. Sci. Technol.* **6**, (1991).
- ²⁹C. L. Littler, D. G. Seiler, and M. R. Loloee, *J. Vac. Soc. A* **8**, 1133 (1990).